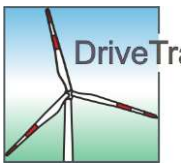

Good Practice Guide

Minimising significant measurement uncertainty contributions from gravity and workpiece clamping

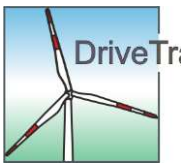

1 Introduction

Gravity causes all workpieces to deflect due to self-weight and also clamping fixtures can cause workpiece deflection. The large components used in renewable energy drive trains are particularly susceptible to deflection due to gravity.

The support method, clamping method and clamping force used can have a significant effect on the resulting workpiece distortion and measurement results but the effect depends on:

- The workpiece geometry.
- The measurement position on the deflected workpiece.
- The effect of distortion on the datum surfaces and thus the definition of the workpiece datum axis.
- The sensitivity of the measurand to both the direct deflection and datum axis definition deviation caused by the deflection.
- The measurement strategy adopted.
- The effect of workpiece deflection during and after the product assembly, ignoring operational load.

There are some effects which are outside the scope of this good practice guide but users of the guide should be aware:

- The measurement uncertainty contribution caused by measuring a workpiece without removal from its manufacturing fixture has not been considered but can be very significant with large thin section workpieces.
- Gravity and clamping deflection also occur during the manufacturing processes, prior to the final inspection of the workpiece. Deflection of the workpiece introduced during manufacturing operations can leave residual effects on workpiece form and thus the measurement strategy (measurement positions and number of measurements) will affect the uncertainty of the measurement result.
- Use of an ‘in-situ’ measuring machine on a manufacturing machine tool, which uses the same rotary datum axis and workpiece clamping arrangement, will result in a contribution to measurement uncertainty caused by elastic deflection when the workpiece is removed from the fixture.
- Thermal effect on clamping forces (as the workpiece changes size) and the effect of friction between the workpiece surface and clamping fixture causing mechanical deflection and also form geometry changes caused by temperature changes.
- Deflection caused by the assembly process and the interface of the workpiece with other components is not discussed in this guide. This can have a significant effect on the function of some renewable drive train components. For example, thin rim bearing assembled shape is deflected by the form deviations in the locating surface- a particularly problem with bearing raceways.

Workpieces used in renewable drive trains vary significantly in size and weight with 200mm to 3000mm diameter components, 100mm face width 2000mm rings and bearings and gears of 50-600mm face widths and weights up to 12000kg. Housings may be asymmetrical and have features which make the orientation on CMMs (co-ordinate measuring machines) used for measurement difficult and prone to deflection under gravity.

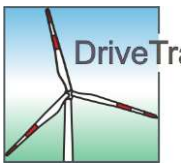

Furthermore, the effect of radial and axial clamping forces during a machining process commonly causes artefacts in the workpiece form which require a properly designed measurement strategy to ensure these effects are properly characterised. The measurement strategy would consider the number and spacing of measurement positons to ensure that the systematic effect from the clamping fixtures can be quantified.

This guide assumes appropriate measuring equipment, with quantified measurement uncertainty, is available and suitable measurement strategies are used.

The impact of these elastic deflections and the measurement uncertainty they introduce depends on the relative size compared to the tolerances specified for the characterising measurands.

2 Minimising deflections caused by gravity

Mounting workpieces on a measuring machine such as a CMM (co-ordinate measuring machine) or GMM (gear measuring machine) usually involves mounting the workpiece directly onto a nominally flat surface or using supports. Common arrangements include:

- Mounting directly onto the CMM worktable. This will result in the lowest deflection caused by gravity of symmetrical workpieces but is prone to dirt and damage to the work table. However with careful application, this may prove the best solution.
- Kinematic support on 3 pads. This assures repeatable location and no redundancy in support, but the resulting deflection can be large with some thin walled components.
- Using > 3pads. This minimises the deflection caused by gravity but is also statically indeterminate if the pad height and workpiece surface form deviations are of similar magnitude to deflections caused by gravity. The resulting deflection may be different with each workpiece.
- Using 3 stiff pads and additional more flexible intermediate support pads to minimise deflection. This has the benefit of a fully kinematic support but has the potential to minimise deflection, if properly designed. It is a complex fixture arrangement and requires careful modelling and validation.

The best way to establish the optimised mounting arrangement is to model the workpiece and mounting arrangement and select the appropriate method based on the results. The model prediction requires a validation and testing to confirm the results.

3 Quantifying deflection caused by gravity and clamping

The deflections are commonly modelled using FEA methods. FEA results are well known for their errors and even a well-defined model which is properly constructed is imperfect. It is common to assume that deviations in modelled deflections of 10% commonly occur and thus even where results are corrected the uncertainty relating to the modelling remains.

The modelling of workpiece general deflection does not necessarily quantify the deviations in the measured surface. In some components, only a proportion of the maximum deflection influences the measurement quantity. Calculating deflection in specific regions or planes is possible in FE packages but is time consuming as you don't know where the maximum deflection occurs until you run the model. Thus it usually requires a series of iterations.

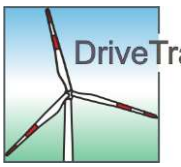

Some example models of workpieces commonly used in wind turbine applications are provided in Annex A. The annex also provides examples of calculated deflection values, which vary between <1µm to 80-90µm and can have a significant effect on the measurement result.

4 Measurement of gravity and clamping effects

An alternative method to quantify the effect of workpiece deflection is to measure the quantities directly with a precision CMM or GMM. The effect of workpiece form and support feature tolerances can be measured directly in a series of tests using the preferred measurement strategy with the orientation of the workpiece systematically changed (rotated for circular workpieces) with respect to the datum fixture and the CMM in order to quantify the effect of different combinations of form deviations. The variation in measured and mean deflection values will quantify the systematic deviations and their uncertainty with the actual CMM/GMM, location fixture and workpiece.

The preferred measurement method is a 3 step process:

- Align the workpiece of the CMM/GMM and perform a minimum of 5 repeat datum surface measurements with a suitable measurement strategy, in order to quantify the datum surface deflected shape and uncertainty of the measuring strategy. Also measure the selected workpiece features to be assessed. This quantifies the machine/workpiece repeatability for datum surface and quantifies both the datum surface and workpiece feature measurement uncertainty.
- Index the workpiece by 45º and measure the datum surface form deviations and selected workpiece features. Keep the location fixtures in the same position on the CMM/GMM if possible. It is recommended that the co-ordinate system is also rotated with the workpiece to minimise the influence from the workpiece datum surface form deviations. Repeat this step until a total of 8 sets of measurements are performed. Smaller indexing intervals may be appropriate for some workpieces.
- Use the mean and standard deviation of the datum surface form to define the deflected shape and the effect of the support method on the selected workpiece features measured. The resulting standard deviation of the measurand will estimate the additional contribution from the workpiece clamping and gravity, although it is acknowledged that other contributions will also be included in this value.

This method estimates both the effect of datum axis definition and workpiece feature uncertainty.

5 Assessment of measurement uncertainty contribution

5.1 General

The influence of elastic deflections from clamping forces and gravity as a result of the workpiece support strategy, workpiece support surface form deviations and tolerances of the support features on measurement uncertainty should be quantified. This should include both:

- Effects on datum axis definition due to deflected datum surfaces. These can be minimised by an appropriate measurement strategy that includes sufficient measurement points and point spacing to include the elastic deflections.
- Effect on the selected measurands.

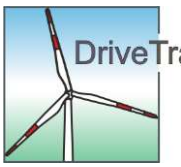

We should consider:

- Systematic deviations in the measurands caused by the deflection. These systematic effects can be used to correct measurement results but remember that no modelling or measurement process is perfect.
- The resulting random variation in the measurand results caused by the measurement strategy from, for example, the measurement position selection with respect to the deflected workpiece.
- Random variation in the measurands caused by the workpiece datum surface form deviations and workpiece support fixture tolerances.
- Uncertainty in the deflection model or measurement process performed on the workpiece. The contributions to measurement uncertainty can be calculated by FEA methods or measured directly with suitable quality CMMs of GMMs.

5.2 Contribution to measurement uncertainty

Quantifying blank deflection due to clamping and gravity effects predicts the elastic distortion of the workpiece but there are 2 additional calculation steps required before the effect on the measurand can be predicted:

- The effect over the measurement range must be quantified. This is difficult to manage in an FE model.
- The deflections (X, Y & Z directions) need to be projected into the normal plane of the measured surface, or in the case of gear measurement, the transverse plane defined in the tolerance standard.

Measurement uncertainty can then be assessed using classical GUM methods (uncertainty budget) or by Monte Carlo simulation methods. The only difficultly with the classical method is estimating the sensitivity coefficient for complex geometry components such as gears and the evaluated parameters. One method of performing this is demonstrated by an example in Annex B for quantifying the influence of gravity when mounting a thin rimmed gear on 3 equally spaced pads on a gear helix deviation parameter $f_{H\beta}$.

The uncertainty budget for the gear example in Annex B without considering deflection due to gravity is shown in Table 1 with an overall uncertainty of ±1.97µm. With the additional influence of gravity, this increases to ±2.80µm as illustrated in Table 2. This is an increase in uncertainty of 41% which is a significant contribution to overall measurement uncertainty. Refer to Annex B for more details on the application of this process.

Table 1 Uncertainty estimate of helix deviation slope $f_{H\beta}$ without elastic deflection

	Uncertainty Source	Units	Value	Dist	Divisor	Ci	n	Ui [µm]
	Calibrated artefact uncertainties							
1	Artefact	µm	1	n	2	1	1	0.500
2	Repeatability of artefact measurement	µm	0.1	n	1	1	5	0.045
3	Uncorrected differences between data	µm	0.4	r	1.732	1	1	0.231
4	Drift of the reference artefact	µm	0	n	1.732	1	1	0.000
5	Difference in artefact Temp. and 20C	ºC	0.3	r	1.732	0.669726	1	0.116
6	Uncertainty in artefact CTE	na	1.16E-06	r	1.732	17320.51	1	0.012
	Work piece uncertainties							
7	Workpiece axial datum error	µm	0.3	r	1.732	0.215	1	0.037
8	Workpiece axial datum uncertainty	µm	0.31	n	1	0.215	1	0.067
9	Workpiece radial datum error	µm	0.3	r	1.732	0.149946	1	0.026
10	Workpiece radial datum uncertainty	µm	0.31	n	1	0.149946	1	0.046
11	Spindle alignment and straighness of Z axis	µm	0.4	r	1.732	1	1	0.231
12	Spindle/Z axis uncertainty	µm	0.31	n	1	1	1	0.310
13	Workpiece form errors	µm	0.2	r	1.732	1	1	0.115
14	Difference in temp. between artefact & 20C	ºC	0.6	r	1.732	1.688345	1	0.585
15	Uncertainty in CTE	na	1.16E-06	r	1.732	87328.18	1	0.058
16	Repeatability of workpiece measurement	µm	0.4	n	1	1	5	0.179
17	Workpiece elastic deflection (z-Axis)	µm	0	r	1.732	0.338481	1	0.000
18	Workpiece elastic deflection (x-y plane)	µm	0	r	1.732	1	1	0.000
19	Elastic deflection model Uncertainty (z-Axis)	µm	0	r	1.732	0.338481	1	0.000
20	Elastic deflection model uncertainty (x-y plane)	µm	0	r	1.732	1	1	0.000
	Descrimination/resolution							
21	System descrimination	µm	0.005	n	2	1	1	0.003
22	Report resolution	µm	0.05	r	1.732	1	1	0.029
	Instrument geometry uncertainties							
23	Rotary-axis uncorrected position errors	rad	4.80E-07	r	1.732	867000	5	0.107
24	Rotary-axis uncertainty	rad	1.50E-06	n	2	867000	5	0.291
	Combined Standard Uncertainty							0.983
	Expanded Uncertainty k=2							**1.965**

Table 2 Uncertainty estimate of helix deviation slope $f_{H\beta}$ with elastic deflection due to gravity

	Uncertainty Source	Units	Value	Dist	Divisor	Ci	n	Ui [µm]
	Calibrated artefact uncertainties							
1	Artefact	µm	1	n	2	1	1	0.500
2	Repeatability of artefact measurement	µm	0.1	n	1	1	5	0.045
3	Uncorrected differences between data	µm	0.4	r	1.732	1	1	0.231
4	Drift of the reference artefact	µm	0	n	1.732	1	1	0.000
5	Difference in artefact Temp. and 20C	ºC	0.3	r	1.732	0.669726	1	0.116
6	Uncertainty in artefact CTE	na	1.16E-06	r	1.732	17320.51	1	0.012
	Work piece uncertainties							
7	Workpiece axial datum error	µm	0.3	r	1.732	0.215	1	0.037
8	Workpiece axial datum uncertainty	µm	0.31	n	1	0.215	1	0.067
9	Workpiece radial datum error	µm	0.3	r	1.732	0.149946	1	0.026
10	Workpiece radial datum uncertainty	µm	0.31	n	1	0.149946	1	0.046
11	Spindle alignment and straighness of Z axis	µm	0.4	r	1.732	1	1	0.231
12	Spindle/Z axis uncertainty	µm	0.31	n	1	1	1	0.310
13	Workpiece form errors	µm	0.2	r	1.732	1	1	0.115
14	Difference in temp. between artefact & 20C	ºC	0.6	r	1.732	1.688345	1	0.585
15	Uncertainty in CTE	na	1.16E-06	r	1.732	87328.18	1	0.058
16	Repeatability of workpiece measurement	µm	0.4	n	1	1	5	0.179
17	Workpiece elastic deflection (z-Axis)	µm	1.8	r	1.732	0.338481	1	0.352
18	Workpiece elastic deflection (x-y plane)	µm	1.6	r	1.732	1	1	0.924
19	Elastic deflection model Uncertainty (z-Axis)	µm	0.2	r	1.732	0.338481	1	0.039
20	Elastic deflection model uncertainty (x-y plane)	µm	0.16	r	1.732	1	1	0.092
	Descrimination/resolution							
21	System descrimination	µm	0.005	n	2	1	1	0.003
22	Report resolution	µm	0.05	r	1.732	1	1	0.029
	Instrument geometry uncertainties							
23	Rotary-axis uncorrected position errors	rad	4.80E-07	r	1.732	867000	5	0.107
24	Rotary-axis uncertainty	rad	1.50E-06	n	2	867000	5	0.291
	Combined Standard Uncertainty							1.397
	Expanded Uncertainty k=2							**2.795**

6 References

ISO 1122-1, Vocabulary of gear terms — Part 1: Definitions related to geometry.

ISO 1328-1:2013, Cylindrical gears- ISO system of flank classification, Part 1: Definitions and allowable values of deviations relevant to the flanks of gear teeth.

ISO/TR 10064-1, Code of inspection practice — Part 1: Inspection of corresponding flanks of gear teeth.

ISO 18653:2003, Gears- Evaluation of instruments for the measurement of individual gears.

ISO 21771, Gears — Cylindrical involute gears and gear pairs — Concepts and geometry.

UKAS M3003 Expression of Uncertainty and Confidence in Measurement (Edition 3, November 2012) http://www.ukas.com/technical-services/publications/publications-relating-to-laboratory-accreditation-3/

VIM International Vocabulary of Metrology – Basic and General Concepts and Associated Terms (VIM 3rd edition) BIPM JCGM 200:2012.

7 Annex A. Example FEA models of drivetrain components

7.1 Introduction

This annex provides examples of deflection models and discussion on the modelling method and typical deflection values. Three examples include:

- Gear blanks
- Thin rimmed bearings
- Asymmetric housing

No FE model is perfect and thus there are uncertainties associated with the predicted deflections. Validation of models by measurement is recommended where practical.

7.2 Example gear model

Figure 1 shows an FEA of a flexible ring gear component with a predicted maximum Z-axis deflection of the datum axis is equal to 6.2µm. This assumes 3 location points in the form of pads or feet. It is assumed the supports and workpiece surface have no form deviations and are frictionless.

Using 6 support points minimises these deflections as illustrated in Figure 2 with a maximum datum surface deflection of 1.9µm but the axis becomes indeterminate because support fixture height tolerances and form tolerances on the workpiece support surfaces will mean that the load sharing cannot be determined. In practice we are unable to determine the load sharing and thus the resulting workpiece deflection with 6 supports may vary between 1.9 and 6.2µm. The uncertainty this will introduce in the datum axis definition will depend on the measurement strategy used to define the datum surface (number of measurement points and point distribution).

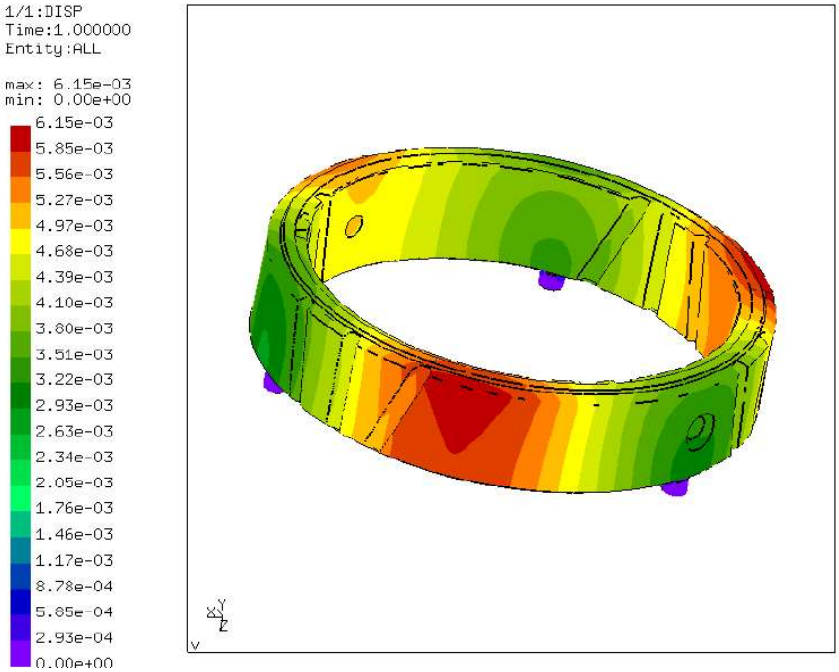

Figure 1 Example of a model of a thin walled workpiece deflection using 3 supports CMI)

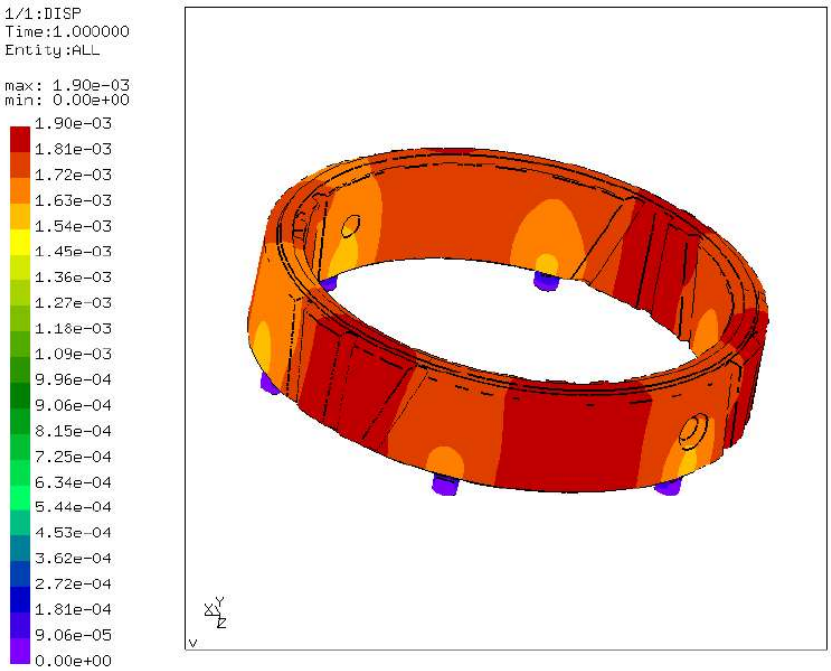

Figure 2 Example of a model of a thin walled workpiece deflection using 6 supports (CMI)

An alternative strategy is to remove the support feet and mount the workpiece directly on the GMM or CMM work table as illustrated in Figure 3. The predicted deflection is at sub-micron

level for two surfaces without form deviations but when form deviations are considered, the prediction of deflection is difficult using FEA methods without specifying the form deviations fully. For this reason many do not use this method.

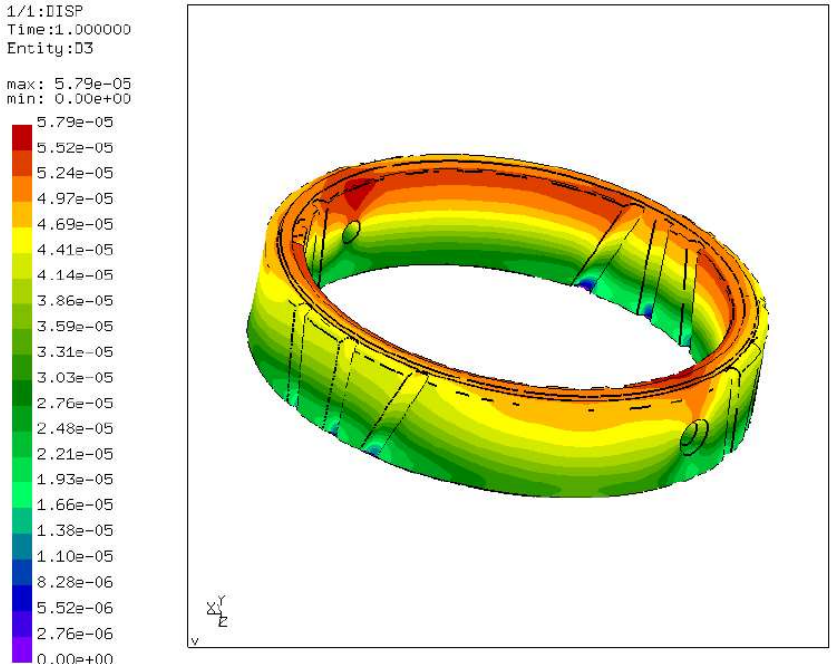

Figure 3 Sub-micron deflections predicted with an error free workpiece mounted directly to an error free reference surface (CMI)

7.3 Thin rim components- bearings

Thin rim components are even more susceptible to deflections due to gravity and clamping force. Many use magnetic blocks to locate the workpiece but this can cause radial distortion of the thin rings if workpieces are moved after the magnetic clamps are locked. Figure 4 illustrates the deflection shape typical of these components.

It is common that the final shape of a thin workpiece is determined not by the component geometry but by the location surfaces that it is mounted on.

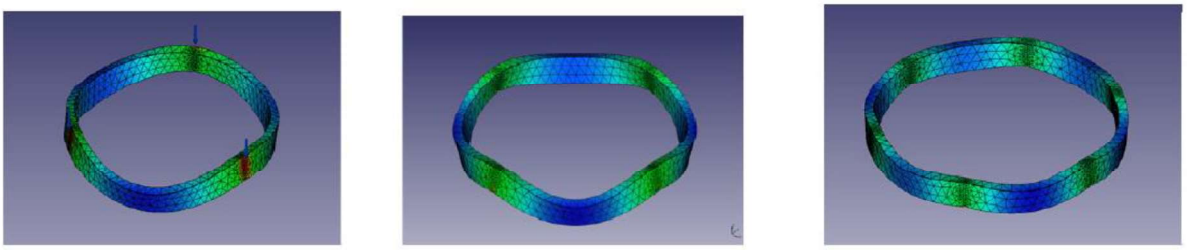

Figure 4 Illustration of a bearing ring type workpiece deflection shape due to gravity (INRIM)

An analysis of 1m diameter ring of height 115mm and thickness 40mm resulted in maximum deflection of 1.9, 0.6 and 0.1µm for 3, 4 and 6 perfect supports and no workpiece form deviations, respectively. A 2m diameter ring of the same section resulted in maximum deflections of 28, 8 and 1.5µm for 3, 4 and 6 supports for the same conditions.

The predicted radial deflection were <0.5µm for the 1m ring and 4.0, 1.5 and 0.3µm for 3, 4 and 6 supports for the 2m ring, respectively.

This example shows that unless the form deviations of the ring and height variation in the datum supports are significantly less than the deflected deviations for the 6 support arrangements, the deflections may approach those of the 4 or 3 support arrangement values.

7.4 Asymmetrical workpieces

An example of an asymmetrical component with varying axial stiffness due to changing cross section represents the most critical component to predict the expected sensitivity due to gravity. A typical example is the wind turbine endplate illustrated in Figure 5. Using 3 supports placed at different orientations relative to the features on the datum surface, shown in Figure 6, results in very different deflections of the clamping face in the vertical axis which can range from 20 to approximately 90µm. This is excessively large compared to the tolerance specification.

Figure 5 Wind turbine gearbox endplate (VTT)

Figure 6 Support feature placement has a significant effect on resulting deflections due to gravity (VTT)

7.5 Summary of FEA estimated workpiece deflections

A summary of the predicted workpiece deflections is provided in Table A1. This quantifies the workpiece blank deflection but does not quantify how the deflection effects the measurement process. This is addressed in Annex B.

Table A1 Summery of FEA predicted workpiece deflections

Component	Dia. [mm]	Facewidth [mm]	Thickness [mm]	Max deflection [µm]	Condition
Ring gear	1980	420	147.5	1.9	6 perfect locating feet/datum surface
				6.2	3 locating feet
				0.06	Perfect datum/mounting surfaces
Bearing ring	1000	115	40	1.9	3 perfect locating feet/datum surface
				0.6	4 perfect locating feet/datum surface
				0.1	6 perfect locating feet/datum surface
Bearing ring	2000	115	40	28	3 perfect locating feet/datum surface
				8.0	4 perfect locating feet/datum surface
				1.5	6 perfect locating feet/datum surface
Asymmetrical component				Various 20-90	

8 Annex B. Estimating measurement uncertainty contribution

8.1 Measurement uncertainty estimate example: helical gear

A large ring type gear artefact from PTB provides a good example of how to estimate the uncertainty caused by elastic deflection due to gravity. The example shown is a gear artefact and as such has limited 'tooth' elements but in a full gear the effect of elastic deflection on tooth geometry will vary around the gear depending on the placement of the support feet and selected measurement positions.

If the support feet and measurement strategy (positions and teeth) are known and fixed for a specific design, the measurement error caused by deflection can be assessed and compensated. The residual measurement uncertainty caused by the modelling uncertainty remains. It is common to assume deflections are within 10-20% of actual values.

The example provides a method of estimating helix and profile measurement uncertainty on a gear and assumes that the feet are spaced at 120^{o} intervals but the orientation relative to the teeth specified in the measurement strategy is random.

8.1.1 Modelling deflections

It is possible to construct an FEA with a projection plane or line to quantify deflections with respect to the orientation of the tooth elements but this requires an iterative process to find the regions of maximum deflection which affect the measurements. A more simple method to quantify the effects is used in this example.

Figures 7, 8 and 9 show the deflection results from an FEA of the ring gear artefact kinematically mounted on 3 location feet for Z, X and Y-axis directions respectively. The Z-axis displacements dominate but do not necessarily generate the largest influence for helix measurement. Helix deviations are measured in the transverse plane and bending effects in that plane are likely to be more significant.

If the gear geometry was a spur gear with helix angle $\beta=0^{o}$, the Z-axis deflections have little effect on helix measurement uncertainty, but as the helix angle of the gear increases, the effect increases (proportionally to $tan\ (\beta_b)$).

The greatest effect is likely to be caused by the bending deflection in the X-Y plane combined with the Z axis deflections, which will be different around the gear. The FEA results need to be evaluated to estimate the effect on helix measurement.

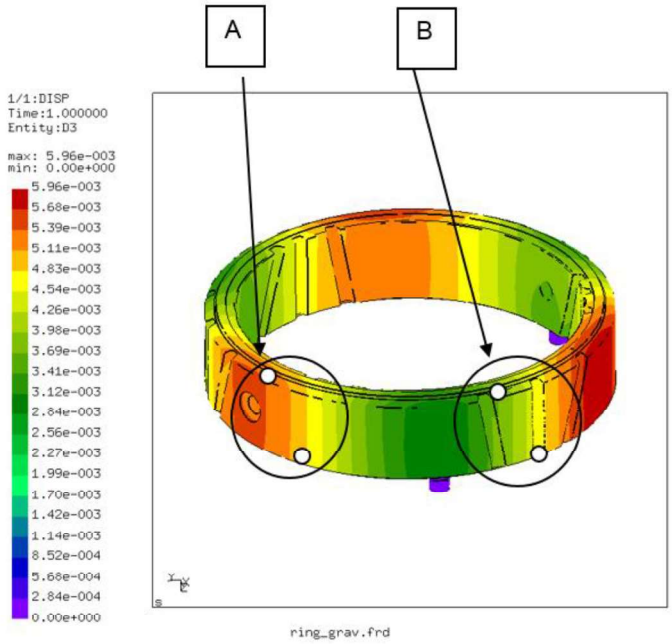

Figure 7 FEA showing regions A and B where the most deflection occurs (CMI)

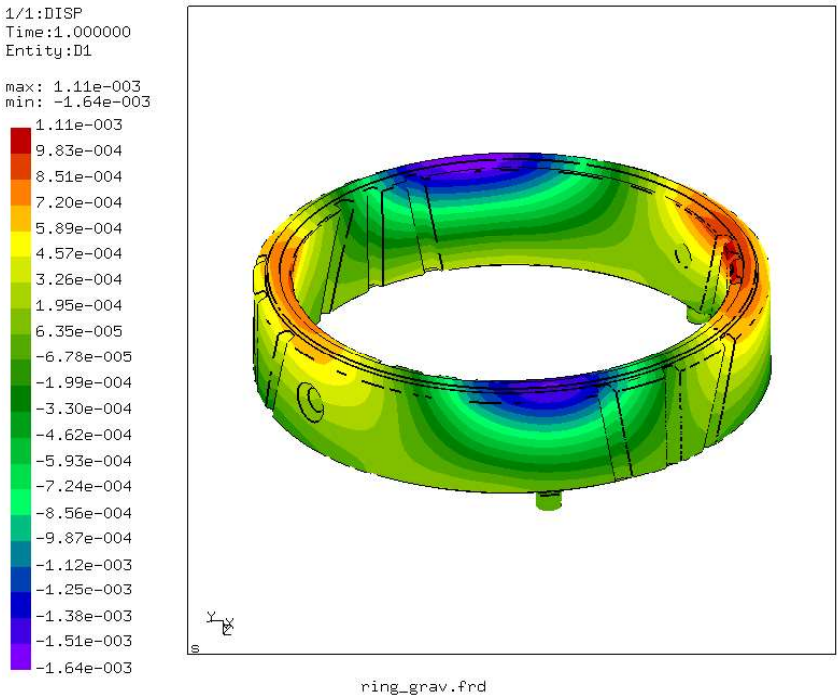

Figure 8 FEA model X- axis displacements (CMI)

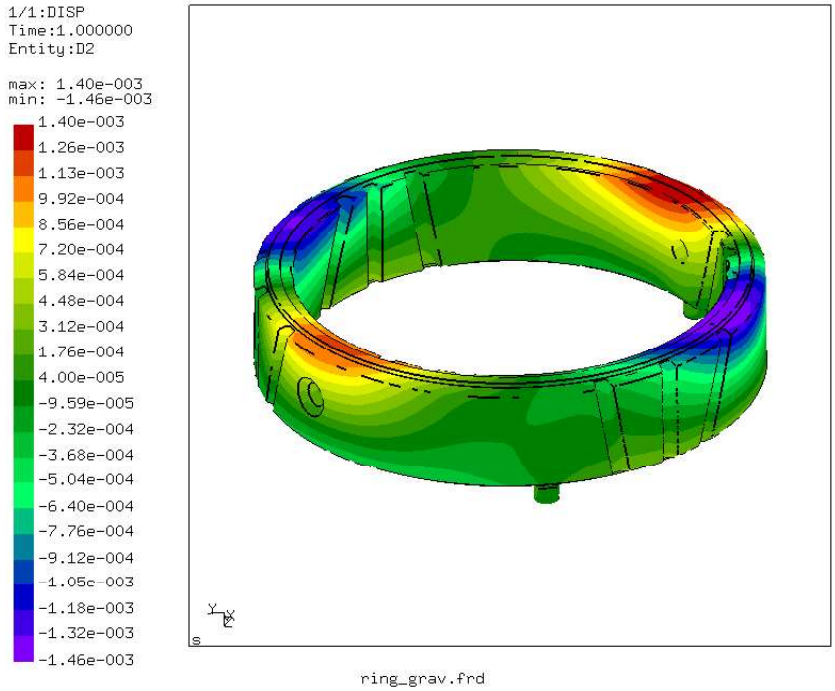

Figure 9 FEA model Y- axis displacements (CMI)

8.1.2 Estimating influence quantities

The X, Y & Z displacements of 2 circles on each end of the gear face width of the gears from Figures 7-9 were extracted by CMI from the FEA model.

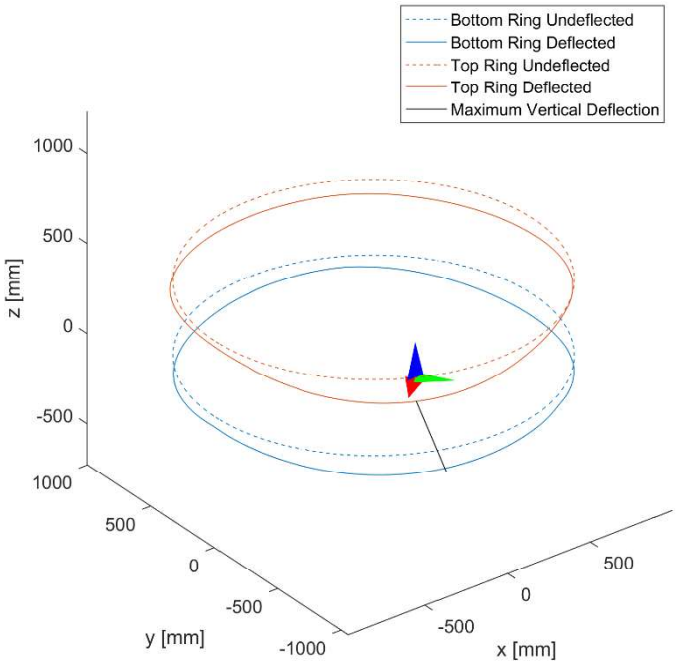

Figure 10 Total deflection of 2 reference circles to estimate relative helix deflection over the face width

Figure 10 shows both the nominal circles (rings) and the total deflections of these circles (X, Y and Z) at the end of the gear face. Figure 10 also shows an example of a single helix line representing a measured left hand helix at the position of maximum predicted vertical deflection. The next step is to convert these end face deflections into estimated deflections over a helical tooth. The effect of deflection on a helix measurement is approximated by the difference in deflection between the upper and lower circles (rings) at each end of the face width. This can be calculated for X, Y and Z directions but for convenience, it is divided into Z direction, tangential direction with respect to the tooth helix (in the helix measurement X-Y plane) and transverse direction to the tooth helix (perpendicular to the helix measurement direction). The helix coordinate system is illustrated in Figure 11. These deflections vary between teeth around the gear because of the support positions.

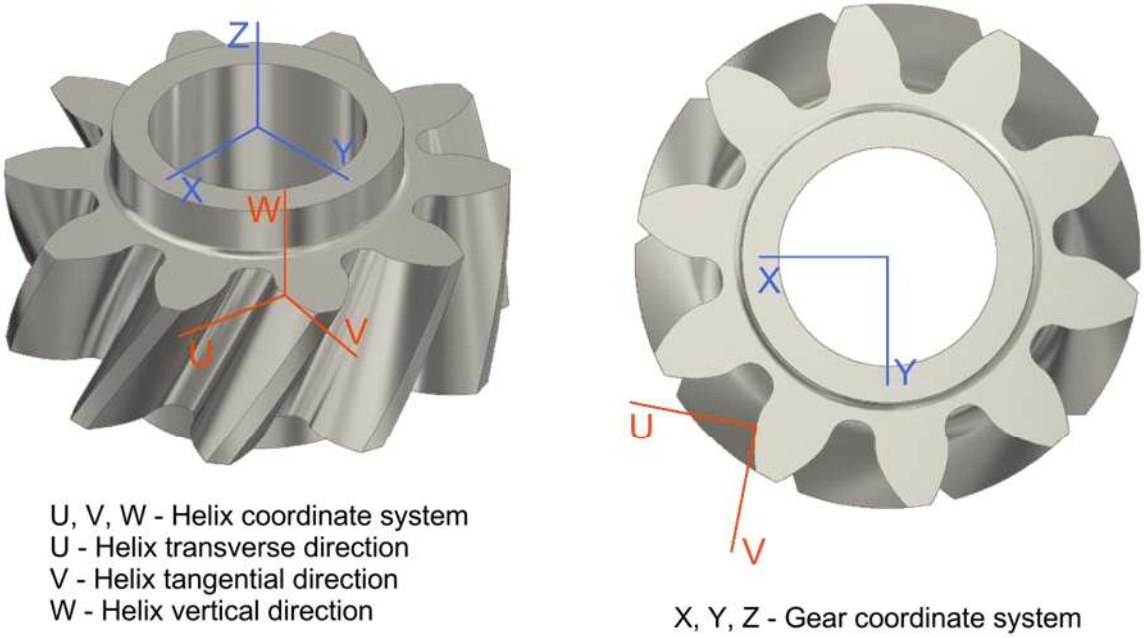

Figure 11 Helix coordinate system

Table B1 Example gear geometry

Gear geometry	
Number of Teeth	101
Normal Module (mm)	18.000
Pressure Angle (degrees)	20.000
Helix Angle (degrees)	±20.000
Reference Diameter (mm)	1934.675
Profile Shift Coefficient.	0.26
Outside Diameter (mm)	1980.04
Root Diameter (mm)	1886.075
Face Width (mm)	420.000
Base Diameter (mm)	1804.075
Active Face Width(mm)	420.000
Base Helix Angle (degrees)	18.747

The difference in deflection from the FEA over a 420mm face width gear with geometry defined in Table B1 is illustrated in Figure 12. The deflection values in Figure 12 are defined as:

- Helix vertical deflection- in the Z-axis direction. This influences the helix measurement result dependent on the gear base helix angle (β_b). For a spur gear, the Z axis deflections have no effect on helix measurement. See Figure 14.
- Helix tangential deflection- in the helix measurement direction. This is in the X-Y plane and directly influences the helix measurement deviation.

- Helix transverse deflection- defined in the X-Y plane, perpendicular to the measurement direction and therefore have a 2nd order influence and these deviations have been ignored in the uncertainty analysis.

Figure 12 shows helix deviation in the tangential (measurement direction) varing between +1.4µm to -1.4µm for a left flank. This is similar to the vertical axis deflection (+1.5µm to -1.3µm). If we compare this to maximum deflections predicted by the FEA model of 5.96µm, the values are significantly smaller. The artefact is non-uniform with both internal and external helix 'gashes' spaced around the ring and thus the deflections are different around the gear.

Figure 13 shows the similar effect on the right flank with a resulting phase shift in the results.

These effects can be compensated as part of the measurement process, provided the position of the deflection is identified with respect to the kinematic support positions. The modelling method is not perfect so there is an uncertainty associated with the correction values, which is likely to be within 10 to 20% of the predicted deflections.

If the position of the supports is unknown, the effects can be considered as random uncertainty from the measurement process if they are uncorrected.

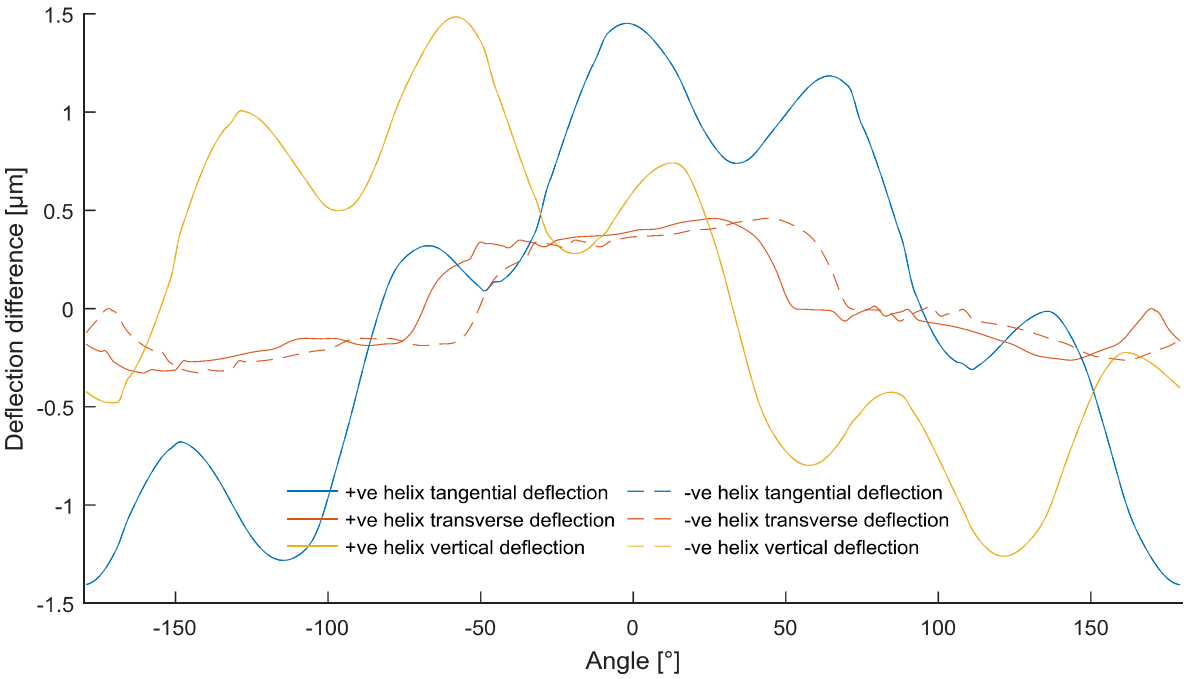

Figure 12 Relative deflection over the 420mm face width gear, in the measurement direction for a left flank.

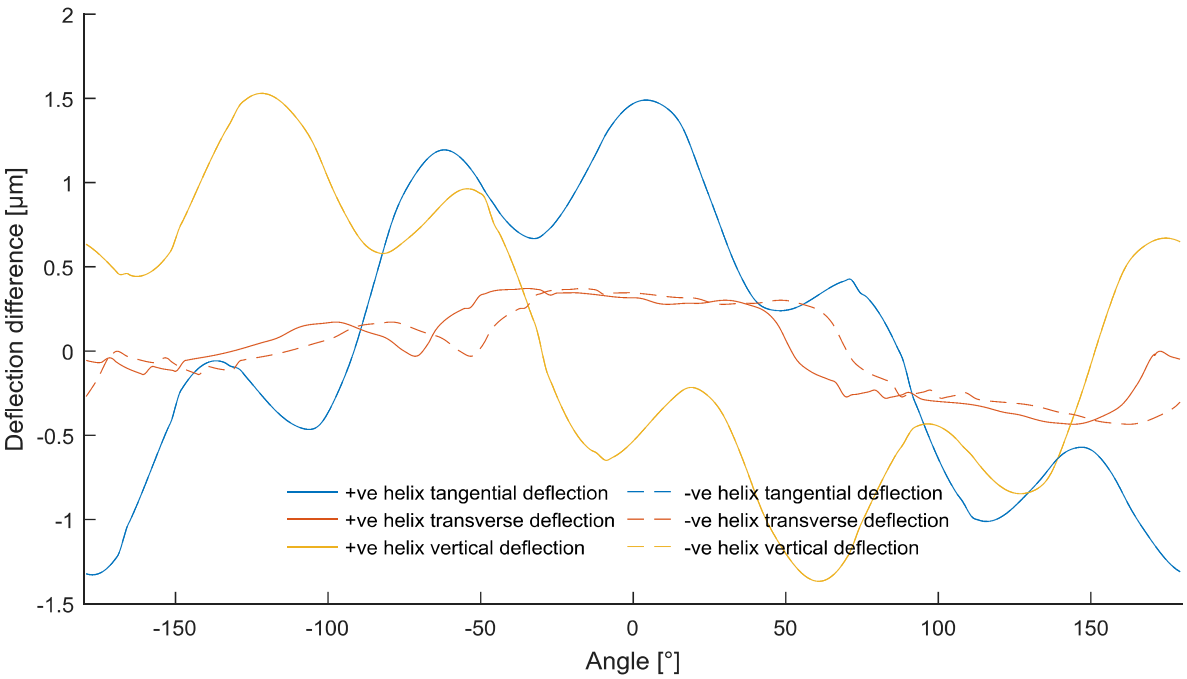

Figure 13 Relative deflection over the 420mm face width gear, in the measurement direction for a right flank.

The effect of the vertical and transverse plane displacements due to gravity of the workpiece on the helix trace depends on the gear geometry. The extent of the influence of the deflection in the vertical axis effects the helix measurement result which is measured in the transverse plane (horizontal axis) will depend on the base helix angle. The relationship is illustrated in Figure 14.

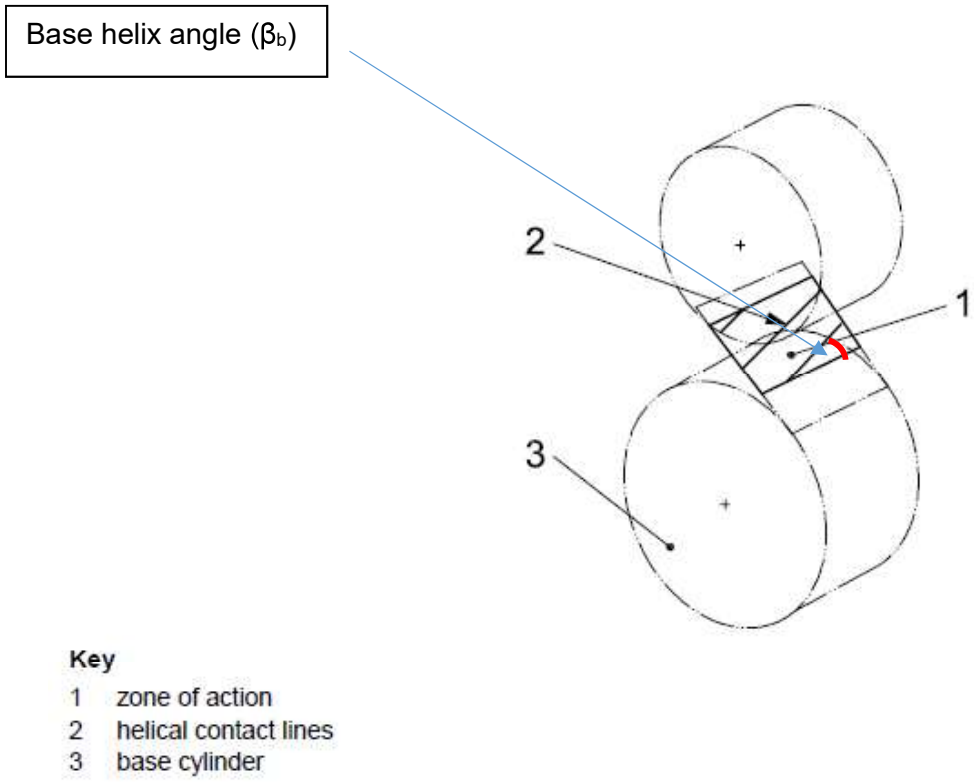

Key

1 zone of action
2 helical contact lines
3 base cylinder

Figure 14 Helical gear plane of contact and base helix angle (from ISO 21771)

The influence of the transverse deflection and the vertical deflection (after accounting for the gear base helix angle) can be combined together into a single deviation and contribution parameter to measurement uncertainty or they can be treated separately.

8.1.3 Example uncertainty budget- helix deviation slope ($f_{H\beta}$)

An uncertainty budget for helix deviation slope measurement uncertainty has been prepared for the example PTB gear artefact in a format consistent with UKAS document M3003. The uncertainty is estimated by a comparator method using a much smaller calibrated artefact as reference artefact. The method is consistent with the recommendation in ISO 18653 and ISO TR 10064-5.

The budget is for a dedicated 4 axis CNC gear measuring machine with a workpiece mounted on a rotary table and a single probe used for datum surface and gear tooth surface measurement. Additional contributions to the measurement uncertainty estimate for large gears include rotary table encoder contributions (as they will be larger than for small calibrated gear used to establish traceability), linear guideway uncertainties (for similar reasons), temperature uncertainties and elastic deflections caused by gravity. Each uncertainty contribution is listed, together with the sensitivity coefficient.

The geometry of both the reference artefact and the workpiece are required to calculate the sensitivity coefficients that estimate the uncertainty contribution to the measurement result, and are summarised in Table B2.

Table B2 summary of reference artefact and workpiece geometry

Artefact Parameters:	Reference	Workpiece
Face width (mm)	125	430
Overall length (mm)	250	430
Length between datum axes/axial datum (mm)	200	2000
Base helix angle (°)	30	18.7
Lead evaluation length (mm)	100	430
Reference diameter (mm)	200	1934

Table B3 shows the uncertainty budget contributions and their descriptions. Other uncertainty models can be constructed and be equally valid, but the key influence factors will be the same.

Table B3 Summary of uncertainty contributions

U_{95} contribution	Description
1	Calibrated reference artefact uncertainty
2	Repeatability using artefact on measuring machine, for 5 tests, indexed at 90º intervals on a rotary table
3	Uncorrected bias between calibration data a mean from 5 measurements
4	Drift in workpiece since last calibration
5	Differences in temperature from 20ºC, When not corrected. Ci value is (coefficient of expansion x evaluation length x Tan(βb))
6	Uncertainty in coefficient of expansion assumed to be 10%
7	Workpiece axial datum definition deviation. Ci is the ratio of axial surface diameter to face width. Rectangular distribution
8	Uncertainty in axial datum definition(measurement process)
9	Workpiece radial datum deviation. Ci is the ratio of eccentricity contribution (from 360º rotation) proportional to the angle of rotation over a helix measurement, which is 0 for spur gears.
10	Uncertainty in radial datum definition. Ci is as (9).
11	Combined spindle (rotary table) alignment and z-axis straightness deviation over the workpiece face width, determined by reference mandrel and reversal method. Ci =1.0.
12	Uncertainty of spindle alignment and reversal method.
13	Workpiece form influence due uncertainty in measurement position. Ci =1.0
14	Uncorrected workpiece temperature deviations. Ci is the (facewidth x Tan(βb)), which is 0 for spur gears.
15	Uncertainty in coefficient of thermal expansion. Ci is the same as (14) but also includes the temperature range of 0.6º.
16	Repeatability of workpiece measurement (in this case 5 times at 90^0 intervals on the rotary table)
17	Workpiece elastic deflection in the z-axis from an FE model or by measurement, assuming these are not corrected. This is rectangular distribution. Ci is the (Tan(βb)), which is 0 for spur gears and 0.338 for the example gear.
18	Workpiece elastic deflection in the x-y plane from an FE model or by measurement, assuming these are not corrected. This is rectangular distribution.
19	Uncertainty of the elastic model used for (17) assumed to by 10%. If the results are corrected, this uncertainty remains and the contribution from (17) is 0. Ci is the (Tan(βb)), which is 0 for spur gears and 0.338 for the example gear.
20	Uncertainty of the elastic model used for (17). If the results are corrected, this uncertainty remains and the contribution from (17) is 0.
21	Estimated measurement discrimination, from tests. Normal distribution and Ci=1.0
22	Report resolution. Rectangular distribution
23	Rotary table calibration: maximum deviations over a typical angle of helix rotation, from calibration data using the rosette method. Ci is the difference between calibrated artefact and workpiece diameter. Rectangular distribution.
24	Maximum uncertainty of the uncorrected rotary table deviations in (23).

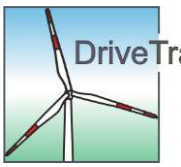

Table B4 Uncertainty estimate of helix deviation slope $f_{H\beta}$ without elastic deflection

	Uncertainty Source	Units	Value	Dist	Divisor	Ci	n	Ui [µm]
	Calibrated artefact uncertainties							
1	Artefact	µm	1	n	2	1	1	0.500
2	Repeatability of artefact measurement	µm	0.1	n	1	1	5	0.045
3	Uncorrected differences between data	µm	0.4	r	1.732	1	1	0.231
4	Drift of the reference artefact	µm	0	n	1.732	1	1	0.000
5	Difference in artefact Temp. and 20C	ºC	0.3	r	1.732	0.669726	1	0.116
6	Uncertainty in artefact CTE	na	1.16E-06	r	1.732	17320.51	1	0.012
	Work piece uncertainties							
7	Workpiece axial datum error	µm	0.3	r	1.732	0.215	1	0.037
8	Workpiece axial datum uncertainty	µm	0.31	n	1	0.215	1	0.067
9	Workpiece radial datum error	µm	0.3	r	1.732	0.149946	1	0.026
10	Workpiece radial datum uncertainty	µm	0.31	n	1	0.149946	1	0.046
11	Spindle alignment and straighness of Z axis	µm	0.4	r	1.732	1	1	0.231
12	Spindle/Z axis uncertainty	µm	0.31	n	1	1	1	0.310
13	Workpiece form errors	µm	0.2	r	1.732	1	1	0.115
14	Difference in temp. between artefact & 20C	ºC	0.6	r	1.732	1.688345	1	0.585
15	Uncertainty in CTE	na	1.16E-06	r	1.732	87328.18	1	0.058
16	Repeatability of workpiece measurement	µm	0.4	n	1	1	5	0.179
17	Workpiece elastic deflection (z-Axis)	µm	0	r	1.732	0.338481	1	0.000
18	Workpiece elastic deflection (x-y plane)	µm	0	r	1.732	1	1	0.000
19	Elastic deflection model Uncertainty (z-Axis)	µm	0	r	1.732	0.338481	1	0.000
20	Elastic deflection model uncertainty (x-y plane)	µm	0	r	1.732	1	1	0.000
	Descrimination/resolution							
21	System descrimination	µm	0.005	n	2	1	1	0.003
22	Report resolution	µm	0.05	r	1.732	1	1	0.029
	Instrument geometry uncertainties							
23	Rotary-axis uncorrected position errors	rad	4.80E-07	r	1.732	867000	5	0.107
24	Rotary-axis uncertainty	rad	1.50E-06	n	2	867000	5	0.291
	Combined Standard Uncertainty							0.983
	Expanded Uncertainty k=2							**1.965**

Table B5 Uncertainty estimate of helix deviation slope $f_{H\beta}$ with elastic deflection

	Uncertainty Source	Units	Value	Dist	Divisor	Ci	n	Ui [µm]
	Calibrated artefact uncertainties							
1	Artefact	µm	1	n	2	1	1	0.500
2	Repeatability of artefact measurement	µm	0.1	n	1	1	5	0.045
3	Uncorrected differences between data	µm	0.4	r	1.732	1	1	0.231
4	Drift of the reference artefact	µm	0	n	1.732	1	1	0.000
5	Difference in artefact Temp. and 20C	ºC	0.3	r	1.732	0.669726	1	0.116
6	Uncertainty in artefact CTE	na	1.16E-06	r	1.732	17320.51	1	0.012
	Work piece uncertainties							
7	Workpiece axial datum error	µm	0.3	r	1.732	0.215	1	0.037
8	Workpiece axial datum uncertainty	µm	0.31	n	1	0.215	1	0.067
9	Workpiece radial datum error	µm	0.3	r	1.732	0.149946	1	0.026
10	Workpiece radial datum uncertainty	µm	0.31	n	1	0.149946	1	0.046
11	Spindle alignment and straighness of Z axis	µm	0.4	r	1.732	1	1	0.231
12	Spindle/Z axis uncertainty	µm	0.31	n	1	1	1	0.310
13	Workpiece form errors	µm	0.2	r	1.732	1	1	0.115
14	Difference in temp. between artefact & 20C	ºC	0.6	r	1.732	1.688345	1	0.585
15	Uncertainty in CTE	na	1.16E-06	r	1.732	87328.18	1	0.058
16	Repeatability of workpiece measurement	µm	0.4	n	1	1	5	0.179
17	Workpiece elastic deflection (z-Axis)	µm	1.8	r	1.732	0.338481	1	0.352
18	Workpiece elastic deflection (x-y plane)	µm	1.6	r	1.732	1	1	0.924
19	Elastic deflection model Uncertainty (z-Axis)	µm	0.2	r	1.732	0.338481	1	0.039
20	Elastic deflection model uncertainty (x-y plane)	µm	0.16	r	1.732	1	1	0.092
	Descrimination/resolution							
21	System descrimination	µm	0.005	n	2	1	1	0.003
22	Report resolution	µm	0.05	r	1.732	1	1	0.029
	Instrument geometry uncertainties							
23	Rotary-axis uncorrected position errors	rad	4.80E-07	r	1.732	867000	5	0.107
24	Rotary-axis uncertainty	rad	1.50E-06	n	2	867000	5	0.291
	Combined Standard Uncertainty							1.397
	Expanded Uncertainty k=2							**2.795**

8.1.4 Results

The uncertainty budgets in Table B4 predicts a helix measurement uncertainty of ±1.965µm without considering elastic deflection of the workpiece due to gravity.

Table B5 shows the same uncertainty budget but with contributions 17-20 included to account for elastic deflection. The resulting uncertainty for helix increases to ±2.795µm, an increase of 41%. Quite a significant increase in measurement uncertainty and as a result, a different mounting arrangement may be considered to minimise the contribution.